Progress In Electromagnetics Research M, Vol. 108, 103–113, 2022

Diffraction of Plane Waves by Arbitrary-Angled Coated Wedges

Giovanni Riccio[1, *], Gianluca Gennarelli,[2], Flaminio Ferrara[3], Claudio Gennarelli[3], and Rocco Guerriero[3]

Abstract—This research work deals with the plane wave diffraction by a coated perfect electrically conducting wedge with arbitrary apex angle. The uniform layer covering the impenetrable wedge is made of a standard double positive material or an unfamiliar double negative metamaterial with negative permittivity and permeability at the operating frequencies. The propagation mechanism is studied when the incidence direction is perpendicular to the edge of the composite structure, and uniform asymptotic solutions are proposed to evaluate the diffraction contribution for both the polarizations. Such approximate solutions are obtained by using the Uniform Asymptotic Physical Optics approach based on electric and magnetic equivalent surface currents radiating in the neighboring free space. The related expressions are user-friendly and provide reliable field values as verified by numerical tests involving a full-wave electromagnetic solver.

1. INTRODUCTION

A coated perfect electrically conducting (PEC) wedge with arbitrary apex angle is positioned in a propagation scenario and modifies the high-frequency electromagnetic field in the surrounding free space by means of the reflection from the surfaces and the diffraction from the edge. This last field contribution is here analyzed in the context of the Uniform Geometrical Theory of Diffraction (UTD) [1] when the considered obstacle is lit by plane waves propagating in the plane orthogonal to the edge (see Fig. 1).

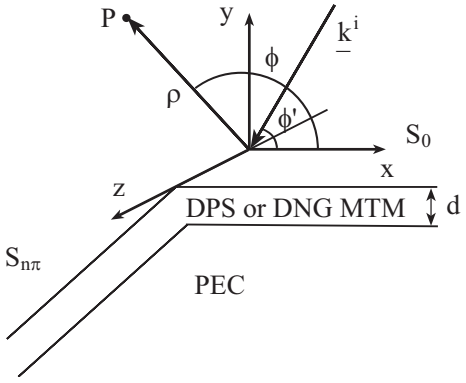

Figure 1. An incident plane wave illuminates a coated PEC wedge with arbitrary apex angle.

Received 4 January 2022, Accepted 8 February 2022, Scheduled 17 February 2022
* Corresponding author: Giovanni Riccio (griccio@unisa.it).
[1] Department of Information and Electrical Engineering and Applied Mathematics, University of Salerno, via Giovanni Paolo II, 132, Fisciano (Salerno) 84084, Italy. [2] Institute for Electromagnetic Sensing of the Environment, National Research Council, via Diocleziano 328, Naples 80124, Italy. [3] Department of Industrial Engineering, University of Salerno, via Giovanni Paolo II, 132, Fisciano (Salerno) 84084, Italy.

The material covering of dielectric and metallic objects is a standard method to alter the electromagnetic scattering of the structure, thus is very attractive in civil and military application areas, e.g., aircrafts and naval ships can require proper material covering of their metallic surfaces to control the radar cross section. The scattering requirements are usually obtained by means of uniform layers made of artificially engineered materials, which can be recognized as double positive (DPS) materials or double negative metamaterials (DNG MTMs) according to the positive or negative values of both the permittivity and permeability at the frequencies of interest. The unusual electromagnetic features of DNG MTMs offer alternative solutions with respect to DPS materials, thus opening new research and application scenarios. Definitions, formulas, and applications of DNG MTMs can be found in many textbooks and research papers available in the open literature (see [2–7] also for other references).

As well known, UTD is an asymptotic analytical approach offering ray tracing representations and allowing high-frequency scattering evaluations more efficient than numerical techniques in real scenarios. If the propagation environment contains coated PEC structures, the UTD peculiarities are exploited for solving two- and three-dimensional scattering problems (heuristic UTD formulations are also included) by taking advantage of impedance boundary conditions (see [8–16] for a partial list of references). Further analytical methods based on the representation of the scattering problem by means of integral equations have been proposed in [17] and [18].

An alternative analytical approach has been proposed for analyzing the diffraction contribution in the UTD framework. The research team has denoted it as Uniform Asymptotic Physical Optics (UAPO) approach since it is based on the PO approximation of electric and magnetic equivalent surface currents radiating in the surrounding region. References [19–31] provide the UAPO solutions to some diffraction problems. Pros and cons of such solutions have been identified and highlighted in these manuscripts. Pros include the opportunity to obtain reliable results, as confirmed by numerical tests and comparisons involving well-assessed numerical techniques, as well as simple formulations in closed form without requiring the solution of differential/integral equations or the calculation of special functions. Cons are essentially associated with the approximate nature of the UAPO solutions. An important role for solving the here tackled diffraction problem has been played by the procedure proposed in [20] with reference to planar junctions made of DPS and DNG MTM layers with PEC backing. In particular, the equivalent transmission line (ETL) models are proposed to evaluate the reflection coefficients for both the polarizations again. This choice is important not only for determining the Geometrical Optics (GO) response of the composite structure (see the next section), but also for formulating the electric and magnetic PO equivalent surface currents in terms of the incident electric field.

2. GO FIELD AND PO SURFACE CURRENTS

Let us consider a plane wave impacting a lossy and uniform layer covering a planar PEC structure (see Fig. 2). The layer has thickness d, permittivity $\varepsilon = \varepsilon_0(\pm\varepsilon' - j\varepsilon'')$, and permeability $\mu = \mu_0(\pm\mu' - j\mu'')$, where ε_0, μ_0 are relevant to the free space; $\varepsilon', \varepsilon'', \mu', \mu''$ are positive quantities; and the sign + or − is associated with DPS or DNG MTM, respectively.

The incident field and that reflected from the external surface of the structure define the GO field contributions at any observation point $P(\underline{r})$ in the free space with impedance ζ_0 and propagation constant k_0. Accounting for the ordinary plane of incidence defined by the unit vector $\hat{k}^i$ of the incidence

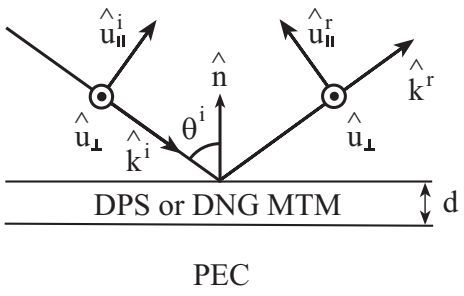

Figure 2. Plane wave reflection from a coated PEC structure.

direction and the unit vector $\hat{n}$ normal to the surface, the incident electric field $\underline{E}^i$ can be expressed in terms of its parallel ($E^i_\parallel$) and perpendicular ($E^i_\perp$) components with respect to such a plane, i.e., $\underline{E}^i = (E^i_\parallel \hat{u}^i_\parallel + E^i_\perp \hat{u}_\perp)\ \mathrm{e}^{-jk_0\hat{k}^i\cdot\underline{r}}$ with $\hat{u}^i_\parallel = \hat{u}_\perp \times \hat{k}^i$ and $\hat{u}_\perp = (\hat{k}^i \times \hat{n})/|\hat{k}^i \times \hat{n}|$ (see Fig. 2). The components of the reflected field $\underline{E}^r = (E^r_\parallel \hat{u}^r_\parallel + E^r_\perp \hat{u}_\perp)\ \mathrm{e}^{-jk_0\hat{k}^r\cdot\underline{r}}$, where $\hat{k}^r$ is the unit vector of the reflection direction and $\hat{u}^r_\parallel = \hat{u}_\perp \times \hat{k}^r$, are related to the incident field components by means of the reflection matrix $\underline{\underline{\Gamma}}$ as follows:

$$\begin{pmatrix} E^r_\parallel \\ E^r_\perp \end{pmatrix} = \begin{pmatrix} \Gamma_\parallel & 0 \\ 0 & \Gamma_\perp \end{pmatrix} \begin{pmatrix} E^i_\parallel \\ E^i_\perp \end{pmatrix} = \underline{\underline{\Gamma}} \begin{pmatrix} E^i_\parallel \\ E^i_\perp \end{pmatrix} \tag{1}$$

The elements of $\underline{\underline{\Gamma}}$ are here determined by using the corresponding ETL models, thus obtaining:

$$\Gamma_{\parallel,\perp} = \frac{Z^{in}_{\parallel,\perp} - Z^0_{\parallel,\perp}}{Z^{in}_{\parallel,\perp} + Z^0_{\parallel,\perp}} \tag{2}$$

where the free-space ETL characteristic impedances are expressed by $Z^0_\parallel = \zeta_0 \cos\theta^i$ and $Z^0_\perp = \zeta_0/\cos\theta^i$, with θ^i being the incidence angle. The ETL input impedances $Z^{in}_{\parallel,\perp}$ account for the thickness and material of the layer, i.e., $Z^{in}_{\parallel,\perp} = jZ_{\parallel,\perp}\tan(k_n d)$ with $Z_\parallel = k_n/(\omega\varepsilon)$, $Z_\perp = (\omega\mu)/k_n$ and $k_n = \pm\beta_n - j\alpha_n$ (k_n is the complex propagation constant associated with $\hat{n}$). Appendix contains useful information about DNG MTM and reflection from a DNG MTM layer with PEC backing.

The knowledge of the GO response of the structure is very important when the UAPO approach is used since it allows one to formulate the PO radiating sources in the approach. The next part of this section is devoted to the evaluation of the electric ($\underline{J}_s$) and magnetic ($\underline{J}_{ms}$) PO equivalent surface currents on S_0 and $S_{n\pi}$ shown in Fig. 1, where the z-axis of a reference system is chosen coincident with the external edge, and the plane $y = 0$ corresponds to the surface S_0 of the structure. The second surface is denoted by $S_{n\pi}$ according to the wedge external angle.

In accordance with the Modified Equivalent Current Approximation (MECA) [32, 33] and the above expressions,

$$\begin{aligned}
\underline{J}_{s_0} &= U_0\left[\hat{n}_{S_0} \times \left(\underline{H}^i + \underline{H}^r\right)\big|_{S_0}\right] \\
&= \frac{U_0}{\zeta_0}\left[\left(1+\Gamma_{\parallel_0}\right)E^i_\parallel \hat{x} + \left(1-\Gamma_{\perp_0}\right)E^i_\perp \sin\phi'\hat{z}\right]\mathrm{e}^{-jk_0\hat{k}^i\cdot\underline{r}'_0} = U_0\underline{J}^*_{s_0}\mathrm{e}^{-jk_0\hat{k}^i\cdot\underline{r}'_0} \qquad (3)\\
\underline{J}_{ms_0} &= U_0\left[\left(\underline{E}^i + \underline{E}^r\right)\big|_{S_0} \times \hat{n}_{S_0}\right] \\
&= U_0\left[-\left(1+\Gamma_{\perp_0}\right)E^i_\perp \hat{x} + \left(1-\Gamma_{\parallel_0}\right)E^i_\parallel \sin\phi'\hat{z}\right]\mathrm{e}^{-jk_0\hat{k}^i\cdot\underline{r}'_0} = U_0\underline{J}^*_{ms_0}\mathrm{e}^{-jk_0\hat{k}^i\cdot\underline{r}'_0} \qquad (4)\\
\underline{J}_{S_{n\pi}} &= U_{n\pi}\left[\hat{n}_{S_{n\pi}} \times \left(\underline{H}^i + \underline{H}^r\right)\big|_{S_{n\pi}}\right] \\
&= \frac{U_{n\pi}}{\zeta_0}\left[-\left(1+\Gamma_{\parallel_{n\pi}}\right)E^i_\parallel\left(\cos(n\pi)\hat{x} + \sin(n\pi)\hat{y}\right) + \left(1-\Gamma_{\perp_{n\pi}}\right)e^i_\perp \sin\left(n\pi - \phi'\right)\hat{z}\right]\mathrm{e}^{-jk_0\hat{k}^i\cdot\underline{r}'_{n\pi}} \\
&= U_{n\pi}\underline{J}^*_{S_{n\pi}}\mathrm{e}^{-jk_0\hat{k}^i\cdot\underline{r}'_{n\pi}} \qquad (5)\\
\underline{J}_{ms_{n\pi}} &= U_{n\pi}\left[\left(\underline{E}^i + \underline{E}^r\right)\big|_{S_{n\pi}} \times \hat{n}_{S_{n\pi}}\right] \\
&= U_{n\pi}\left[\left(1+\Gamma_{\perp_{n\pi}}\right)E^i_\perp\left(\cos(n\pi)\hat{x} + \sin(n\pi)\hat{y}\right) + \left(1-\Gamma_{\parallel_{n\pi}}\right)E^i_\parallel \sin\left(n\pi - \phi'\right)\hat{z}\right]\mathrm{e}^{-jk_0\hat{k}^i\cdot\underline{r}'_{n\pi}} \\
&= U_{n\pi}\underline{J}^*_{ms_{n\pi}}\mathrm{e}^{-jk_0\hat{k}^i\cdot\underline{r}'_{n\pi}} \qquad (6)
\end{aligned}$$

wherein $\hat{k}^i = -\cos\phi'\hat{x} - \sin\phi'\hat{y}$, $\underline{r}'_{0,n\pi}$ denotes the source point $P'(\underline{r}')$, and $U_{0,n\pi}$ is equal to 1 or 0 depending on the ON/OFF illumination of the related surface by the incident plane wave. This last point is strictly related to the PO approximation and limits the evaluation of the scattered field at the beginning of the UAPO approach. It is authors' opinion that the inclusion of further wave

contributions can improve the formulation of the equivalent surface currents to be used also in the shadow region, but this means abandoning the simplicity of the PO approximation and probably preventing the determination of a UTD-like solution in closed form as in [19–31].

3. UAPO DIFFRACTED FIELD

The electric and magnetic PO equivalent surface currents on S_0 and $S_{n\pi}$ are now used to apply the UAPO approach. As a matter of fact, they act as radiating sources in the radiation integral to evaluate the scattered field $\underline{E}^s$, i.e.,

$$\begin{aligned}\underline{E}^s \;=\; & -jk_0 \iint\limits_{S_0} \left[\left(\underline{\underline{I}} - \hat{R}_0\hat{R}_0\right)\zeta_0\underline{J}_{s_0} + \underline{J}_{ms_0}\times\hat{R}_0\right]\frac{\mathrm{e}^{-jk_0R_0}}{4\pi R_0}\mathrm{d}S_0 \\ & -jk_0 \iint\limits_{S_{n\pi}} \left[\left(\underline{\underline{I}} - \hat{R}_{n\pi}\hat{R}_{n\pi}\right)\zeta_0\underline{J}_{s_{n\pi}} + \underline{J}_{ms_{n\pi}}\times\hat{R}_{n\pi}\right]\frac{e^{-jk_0R_{n\pi}}}{4\pi R_{n\pi}}\mathrm{d}S_{n\pi}\end{aligned} \tag{7}$$

where $\underline{\underline{I}}$ is the 3×3 identity matrix, $R_{0,n\pi} = |\underline{r} - \underline{r}'_{0,n\pi}|$ and $\hat{R}_{0,n\pi} = (\underline{r} - \underline{r}'_{0,n\pi})/R_{0,n\pi}$. Note that the linearity of the radiation integral permits to separate the contribution of each surface.

Since the source point of the diffracted field is on the edge, the approximation $\hat{R}_{0,n\pi} \cong \hat{\rho} = \cos\phi\hat{x} + \sin\phi\hat{y}$ is permitted in the square brackets, thus obtaining

$$\underline{E}^s \cong U_0\left[(\underline{\underline{I}} - \hat{\rho}\hat{\rho})\zeta_0\underline{J}^*_{s_0} + \underline{J}^*_{ms_0}\times\hat{\rho}\right]I_0^s + U_{n\pi}\left[(\underline{\underline{I}} - \hat{\rho}\hat{\rho})\zeta_0\underline{J}^*_{s_{n\pi}} + \underline{J}^*_{ms_{n\pi}}\times\hat{\rho}\right]I_{n\pi}^s \tag{8}$$

with

$$I^s_{0,n\pi} = \frac{-jk_0}{4\pi}\iint \frac{\mathrm{e}^{-jk_0\left(\hat{k}^i\cdot\,\underline{r}'_{0,n\pi} + |\underline{r}-\underline{r}'_{0,n\pi}|\right)}}{\left|\underline{r} - \underline{r}'_{0,n\pi}\right|}\,\mathrm{d}S_{0,n\pi} \tag{9}$$

Accounting for useful approximations, mathematical computations, integral representations, and asymptotic evaluations (see [20] as reference for the analytical procedure), it is possible to extract the diffraction contributions $I^d_{0,n\pi}$ composed in Eq. (9). They can be so expressed:

$$I_0^d = \frac{\mathrm{e}^{-j\pi/4}}{2\sqrt{2\pi k_0}}\frac{F_t\left(2k_0\rho\cos^2\left(\dfrac{\phi\pm\phi'}{2}\right)\right)}{\cos\phi + \cos\phi'}\frac{\mathrm{e}^{-jk_0\rho}}{\sqrt{\rho}} \tag{10}$$

$$I_{n\pi}^d = \frac{\mathrm{e}^{-j\pi/4}}{2\sqrt{2\pi k_0}}\frac{F_t\left(2k_0\rho\cos^2\left(\dfrac{(n\pi-\phi)\pm(n\pi-\phi')}{2}\right)\right)}{\cos(n\pi-\phi) + \cos(n\pi-\phi')}\frac{\mathrm{e}^{-jk_0\rho}}{\sqrt{\rho}} \tag{11}$$

in which ρ is the radial distance of P, and $F_t(\cdot)$ is the UTD transition function [1]. The use of the sign $+$ or $-$ in Eqs. (10) and (11) depends on the position of P with respect to S_0 and $S_{n\pi}$. In fact, $+(-)$ must be considered in Eq. (10) if $0 < \phi < \pi(\pi < \phi < n\pi)$ and in Eq. (11) if $(n-1)\pi < \phi < n\pi(0 < \phi < (n-1)\pi)$.

The UAPO diffracted field then results from Eq. (8) as follows:

$$\underline{E}^d = U_0\left[(\underline{\underline{I}} - \hat{\rho}\hat{\rho})\zeta_0\underline{J}^*_{s_0} + \underline{J}^*_{ms_0}\times\hat{\rho}\right]I_0^d + U_{n\pi}\left[(\underline{\underline{I}} - \hat{\rho}\hat{\rho})\zeta_0\underline{J}^*_{s_{n\pi}} + \underline{J}^*_{ms_{n\pi}}\times\hat{\rho}\right]I_{n\pi}^d \tag{12}$$

It can be conveniently expressed according to the two-dimensional UTD formulation, i.e.,

$$\underline{E}^d = \begin{pmatrix} E_z^d \\ E_\phi^d \end{pmatrix} = \underline{\underline{D}}\begin{pmatrix} E_z^i \\ E_{\phi'}^i \end{pmatrix}\frac{\mathrm{e}^{-jk_0\rho}}{\sqrt{\rho}} \tag{13}$$

where the UAPO diffraction matrix D is written as:

$$\underline{\underline{D}} = \begin{pmatrix} D_{zz} & 0 \\ 0 & D_{\phi\phi'} \end{pmatrix} = U_0\begin{pmatrix} D_{zz_0} & 0 \\ 0 & D_{\phi\phi'_0} \end{pmatrix} + U_{n\pi}\begin{pmatrix} D_{zz_{n\pi}} & 0 \\ 0 & D_{\phi\phi'_{n\pi}} \end{pmatrix} = U_0\underline{\underline{D}}_0 + U_{n\pi}\underline{\underline{D}}_{n\pi} \tag{14}$$

with

$$D_{zz_0} = \frac{\mathrm{e}^{-j\pi/4}}{2\sqrt{2\pi k_0}}\left[(1-\Gamma_{\perp_0})\sin\phi' - (1+\Gamma_{\perp_0})\sin\phi\right]\frac{F_t\left(2k_0\rho\cos^2\left(\dfrac{\phi\pm\phi'}{2}\right)\right)}{\cos\phi+\cos\phi'} \tag{15}$$

$$D_{\phi\phi'_0} = \frac{\mathrm{e}^{-j\pi/4}}{2\sqrt{2\pi k_0}}\left[\left(1+\Gamma_{\parallel_0}\right)\sin\phi - \left(1-\Gamma_{\parallel_0}\right)\sin\phi'\right]\frac{F_t\left(2k_0\rho\cos^2\left(\dfrac{\phi\pm\phi'}{2}\right)\right)}{\cos\phi+\cos\phi'} \tag{16}$$

$$D_{zz_{n\pi}} = \frac{\mathrm{e}^{-j\pi/4}}{2\sqrt{2\pi k_0}}\left[(1-\Gamma_{\perp_{n\pi}})\sin(n\pi-\phi')-(1+\Gamma_{\perp_{n\pi}})\sin(n\pi-\phi)\right]\frac{F_t\left(2k_0\rho\cos^2\left(\dfrac{(n\pi-\phi)\pm(n\pi-\phi')}{2}\right)\right)}{\cos(n\pi-\phi)+\cos(n\pi-\phi')} \tag{17}$$

$$D_{\phi\phi'_{n\pi}} = \frac{\mathrm{e}^{-j\pi/4}}{2\sqrt{2\pi k_0}}\left[\left(1+\Gamma_{\parallel_{n\pi}}\right)\sin(n\pi-\phi)-\left(1-\Gamma_{\parallel_{n\pi}}\right)\sin(n\pi-\phi')\right]\frac{F_t\left(2k_0\rho\cos^2\left(\dfrac{(n\pi-\phi)\pm(n\pi-\phi')}{2}\right)\right)}{\cos(n\pi-\phi)+\cos(n\pi-\phi')} \tag{18}$$

Note that Eqs. (13) and (14) are obtained with no "a priori" limitations on geometric, electric, and magnetic parameters of the involved layers. Of course, they account only for the presence of the external wedge and neglect the field interactions with the inner PEC wedge.

4. NUMERICAL EXAMPLES

Tests showing the UAPO field ability to balance the discontinuities of the GO field across the shadow boundaries and to provide reliable values are presented in this section when $\phi' = \pi/3$ and $\rho = 7\lambda_0$, with λ_0 being the free-space wavelength.

Figures 3 and 4 show the GO and UAPO field contributions as well as the total fields when considering a wedge identified by $n = 1.2$ and a DPS covering with $\varepsilon/\varepsilon_0 = 2.3 - j0.023$, $\mu/\mu_0 = 1$ and $d = 0.1\lambda_0$. Based on the incidence direction, both the surfaces are lit by the incident plane wave ($U_{0,n\pi} = 1$) and contribute to the UAPO field associated with the parallel (see Fig. 3) and perpendicular

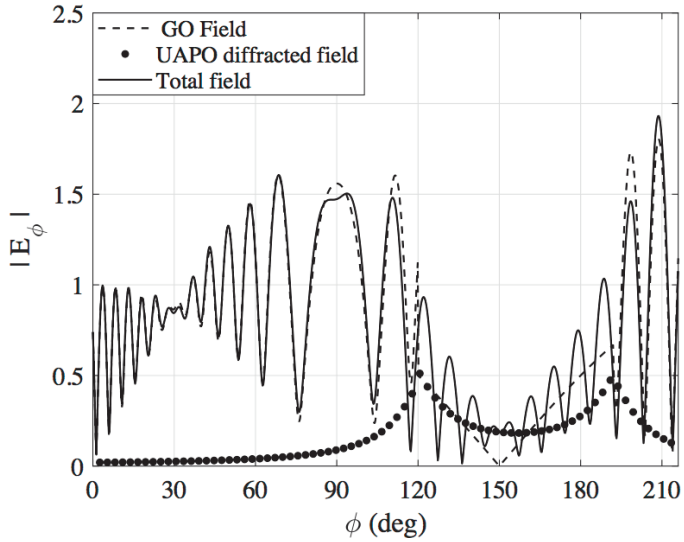

Figure 3. Incident plane wave with parallel polarization ($E_z^i = 0$, $E_{\phi'}^i = 1$). Wedge with $n = 1.2$ and DPS covering with $\varepsilon/\varepsilon_0 = 2.3 - j0.023$, $\mu/\mu_0 = 1$, $d = 0.1\lambda_0$.

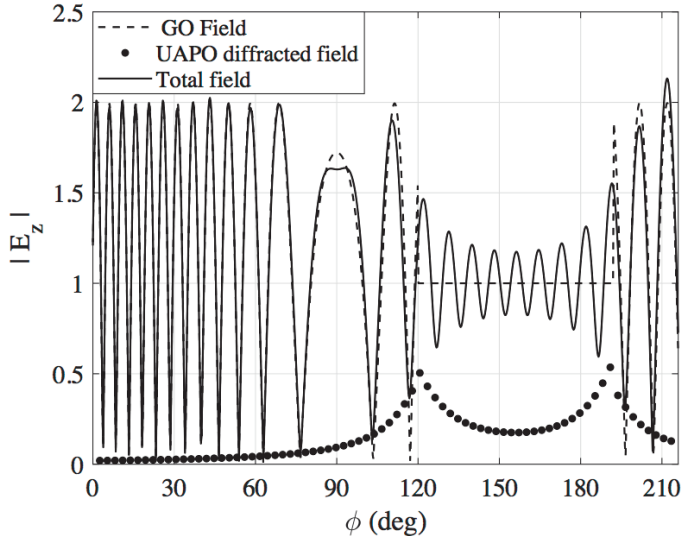

Figure 4. Incident plane wave with perpendicular polarization ($E_z^i = 1$, $E_{\phi'}^i = 0$). Wedge with $n = 1.2$ and DPS covering with $\varepsilon/\varepsilon_0 = 2.3 - j0.023$, $\mu/\mu_0 = 1$, $d = 0.1\lambda_0$.

(see Fig. 4) polarizations. An angular region of about seventy degrees separates the reflection boundaries, where jumps of the GO field and peaks of the UAPO field exist. Obviously, different field levels result in the first (from S_0 to the first reflection boundary) and third (from the second reflection boundary to $S_{n\pi}$) angular regions, since different values of the reflection coefficients exist. Moreover, it is necessary to take into account that the output unit vector $\hat{\phi}$ changes in direction when P moves and then $E_{\phi}^i \neq E_{\phi'}^i$. The continuity of the total fields in Figs. 3 and 4 certifies the UAPO field ability to compensate the GO field discontinuities as expected.

The accuracy of the UAPO solution is now tested by using the RF module of Comsol Multiphysics®, which relies heavily on the proven Finite Element Method (FEM). In particular, Fig. 5 continues the analysis opened by Fig. 4 with $E_z^i = 1$, $E_{\phi'}^i = 0$ and shows: a) the amplitude of the UAPO-based total field and the Comsol Multiphysics® counterpart; b) the comparison between the phase values; c) the amplitude of the UAPO diffracted field and the amplitude of the Comsol Multiphysics® data deprived of the GO field. The agreements in Figs. 5(a) and 5(b) are very good, thus assessing

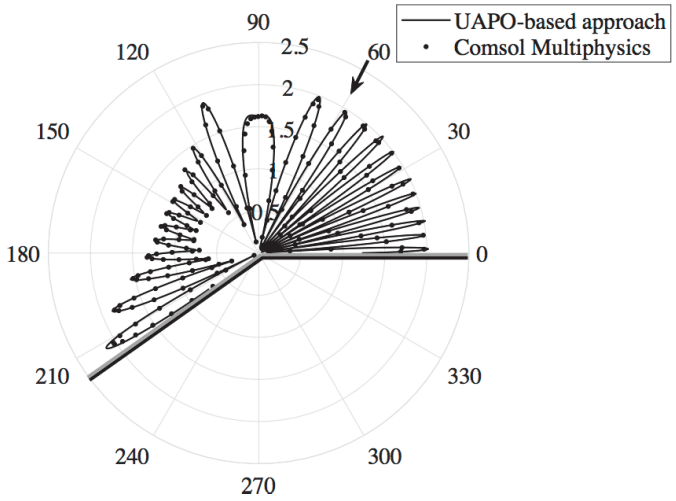

(a)

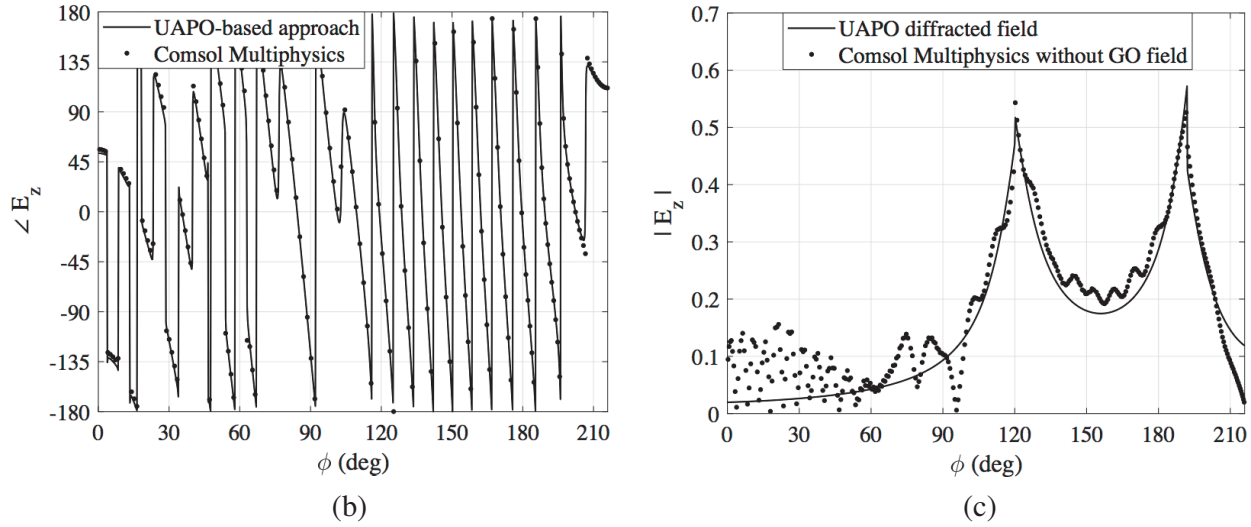

Figure 5. Incident plane wave with perpendicular polarization ($E_z^i = 1$, $E_{\phi'}^i = 0$). Wedge with $n = 1.2$ and DPS covering with $\varepsilon/\varepsilon_0 = 2.3 - j0.023$, $\mu/\mu_0 = 1$, $d = 0.1\lambda_0$.

the efficacy of the UAPO approach, and the comparison in Fig. 5(c) is acceptable, since it confirms the relevance of the diffraction by the outer dielectric wedge and makes evident the presence of other contributions (e.g., terms due to the propagation of the diffraction by the inner PEC wedge), which are not considered in the proposed approach. The results in Fig. 6 are relevant to an increased thickness of the DPS layer, i.e., $d = 0.5\lambda_0$, and recommend limiting the approach to thin layers compared to λ_0. Such a recommendation is also suggested by further comparisons corresponding to $d > 0.5\lambda_0$. Fig. 7 permits to estimate the reliability of the UAPO-based results when only one surface is lit by the incident wave. As a matter of fact, $S_{n\pi}$ is in the shadow region ($U_{n\pi} = 0$) by choosing $n = 1.7$ and $\phi' = \pi/3$, so that only S_0 contributes to the UAPO diffracted field. The comparison confirms the very good performance also in this case.

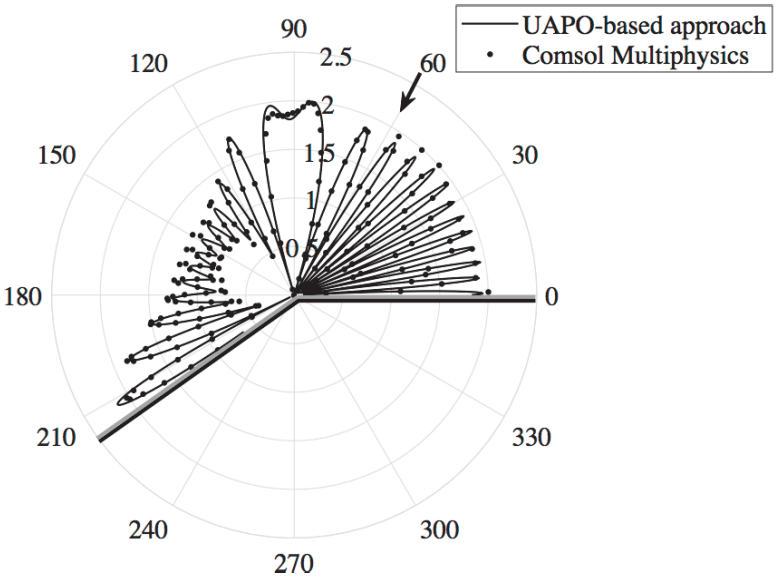

Figure 6. Incident plane wave with perpendicular polarization ($E_z^i = 1$, $E_{\phi'}^i = 0$). Wedge with $n = 1.2$ and DPS covering with $\varepsilon/\varepsilon_0 = 2.3 - j0.023$, $\mu/\mu_0 = 1$, $d = 0.5\lambda_0$.

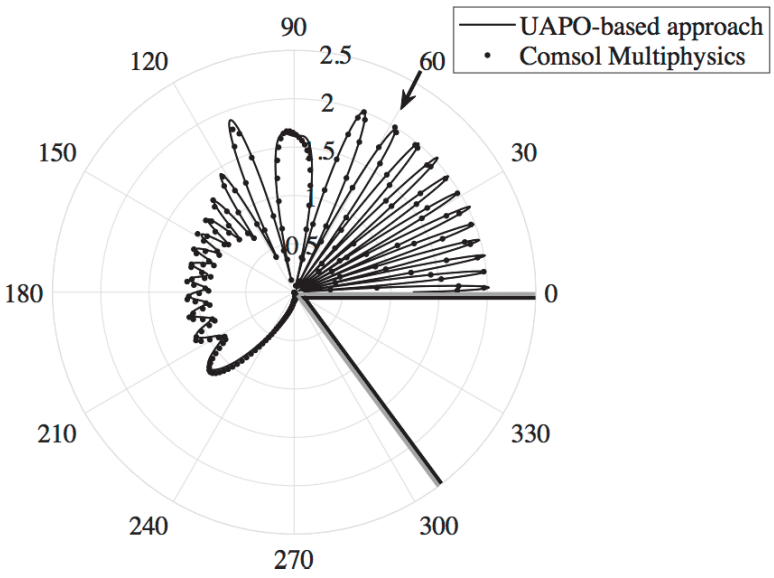

Figure 7. Incident plane wave with perpendicular polarization ($E_z^i = 1$, $E_{\phi'}^i = 0$). Wedge with $n = 1.7$ and DPS covering with $\varepsilon/\varepsilon_0 = 2.3 - j0.023$, $\mu/\mu_0 = 1$, $d = 0.1\lambda_0$.

Figures 8 and 9 show what changes with respect to Figs. 5 and 7, respectively, when using the sign minus in front of the real part of permittivity and permeability, i.e., the coating now possesses DNG MTM characteristics. The agreements are very good, thus endorsing the effectiveness of the proposed approach.

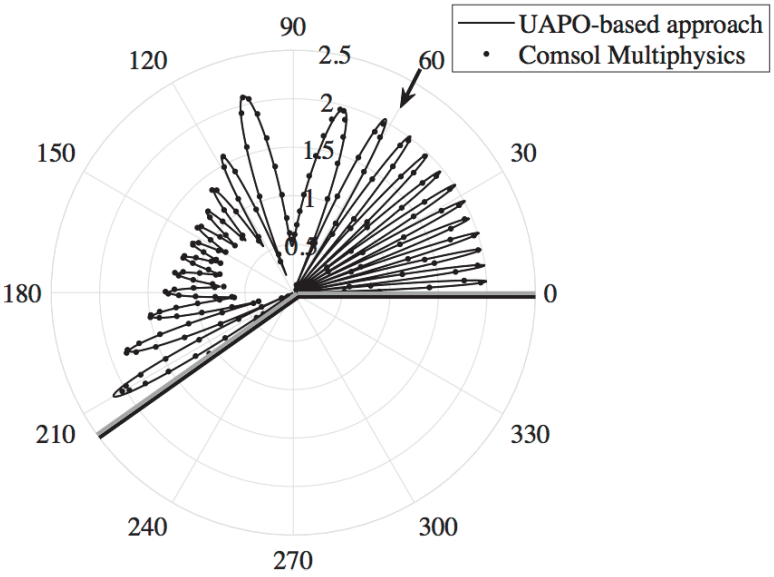

Figure 8. Incident plane wave with perpendicular polarization ($E_z^i = 1$, $E_{\phi'}^i = 0$). Wedge with $n = 1.2$ and DNG MTM covering with $\varepsilon/\varepsilon_0 = -2.3 - j0.023$, $\mu/\mu_0 = -1$, $d = 0.1\lambda_0$.

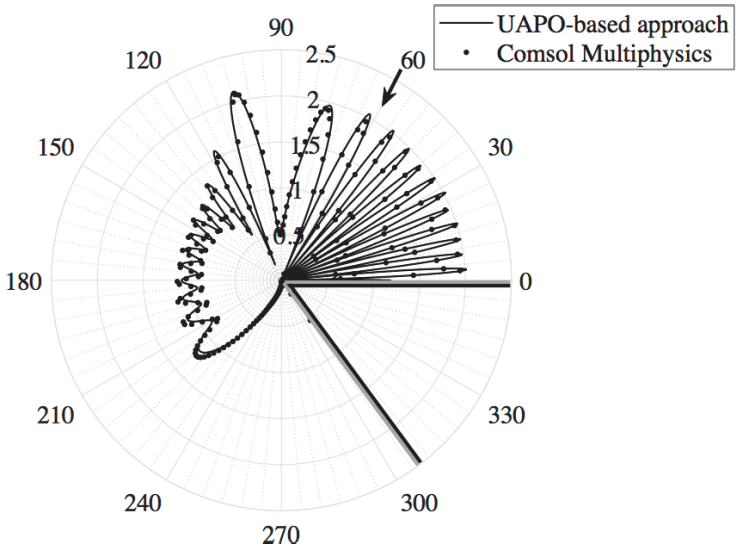

Figure 9. Incident plane wave with perpendicular polarization ($E_z^i = 1$, $E_{\phi'}^i = 0$). Wedge with $n = 1.7$ and DNG MTM covering with $\varepsilon/\varepsilon_0 = -2.3 - j0.023$, $\mu/\mu_0 = -1$, $d = 0.1\lambda_0$.

5. CONCLUDING REMARKS

Comparisons with Comsol Multiphysics® results concerning DPS or DNG MTM coatings prove the effectiveness of the proposed UAPO approach for the plane wave diffraction by an arbitrary-angled coated wedge. The corresponding solution is in closed form and conveniently formulated in the UTD framework. Moreover, it must be marked that the agreement with the Comsol Multiphysics® data decreases by increasing the thickness with respect to the wavelength and that the inclusion of the field interactions with the inner PEC wedge can produce better results.

APPENDIX A.

DNG MTMs exhibit simultaneously negative real parts of both permittivity and permeability, and are also commonly referred as negative index materials (NIMs) or left-handed materials (LHMs) or backward (BW) media accounting for their unusual characteristics. In fact, the term NIM is related to the corresponding refraction index with negative real part thus leading to anomalous refraction properties, whereas the term LHM makes evident that electric field, magnetic field, and wave vector of a propagating plane wave obey the left-hand rule rather than the right-hand one, as it occurs in conventional media, and the term BW means that the backward wave propagation characterized by the wave vector antiparallel to the Poynting one is supported. DNG MTMs are artificially engineered materials obtained by embedding small inclusions in host media.

When a uniform plane wave propagating in free space impinges on a planar DNG MTM interface, the Snell's law of reflection continues to be valid by returning specular propagation, whereas the Snell's law of refraction implies a negative refraction angle. This last occurrence means that the transmitted wave propagates in the same side with respect to the normal to the interface. Accounting for this propagation effect, when a DNG MTM layer with PEC backing is lit by an incident plane wave, it is possible to evaluate the reflection coefficients for parallel and perpendicular polarizations by means of the ETL formulation (2), where the complex propagation constant $k_n = -\beta_n - j\alpha_n$ associated with the normal to the interface is defined by [20]:

$$\beta_n = \sqrt{\frac{\sqrt{A^2 + \left[B - (k_0 \sin\theta^i)^2\right]^2} + B - (k_0 \sin\theta^i)^2}{2}} \tag{A1}$$

$$\alpha_n = \sqrt{\frac{\sqrt{A^2 + \left[B - (k_0 \sin\theta^i)^2\right]^2} - B + (k_0 \sin\theta^i)^2}{2}} \tag{A2}$$

with $A = k_0^2(\varepsilon'\mu'' + \varepsilon''\mu')$ and $B = k_0^2(\varepsilon'\mu' - \varepsilon''\mu'')$.

REFERENCES

1. Kouyoumjian, R. G. and P. H. Pathak, "A uniform geometrical theory of diffraction for an edge in a perfectly conducting surface," *Proc. IEEE*, Vol. 62, 1448–1461, 1974.
2. Engheta, N. and R. W. Ziolkowski, editors, *Metamaterials: Physics and Engineering Explorations*, Wiley & Sons, USA, 2006.
3. Marquéz, R., F. Martin, and M. Sorolla, *Metamaterials with Negative Parameters: Theory, Design and Microwave Applications*, Wiley & Sons, USA, 2008.
4. Sakoda, K., editor, *Electromagnetic Metamaterials: Modern Insights into Macroscopic Electromagnetic Fields*, Springer, Singapore, 2019.
5. Kong, J. A., "Electromagnetic wave interaction with stratified negative isotropic media," *Progress In Electromagnetics Research*, Vol. 35, 1–52, 2002.
6. Chew, W. C., "Some reflections on double negative materials," *Progress In Electromagnetics Research*, Vol. 51, 1–26, 2005.
7. Basdemir, H. D., "Diffraction by a right angle impedance wedge between left- and right-handed media," *Journal of Electromagnetic Waves and Applications*, Vol. 34, No. 7, 869–880, 2020.
8. Tiberio, R., G. Pelosi, and G. Manara, "A uniform GTD formulation for the diffraction by a wedge with impedance faces," *IEEE Trans. Antennas Propag.*, Vol. 33, 867–873, 1985.
9. Senior, T. B. A. and J. L. Volakis, "Scattering by an imperfect right-angled wedge," *IEEE Trans. Antennas Propag.*, Vol. 34, 681–689, 1986.
10. Rojas, R. G., "Electromagnetic diffraction of an obliquely incident plane wave field by a wedge with impedance faces," *IEEE Trans. Antennas Propag.*, Vol. 36, 956–970, 1988.
11. Syed, H. H. and J. L. Volakis, "An approximate solution for scattering by an impedance wedge at skew incidence," *Radio Sci.*, Vol. 3, 505–524, 1995.
12. Osipov, A. V. and T. B. A. Senior, "Diffractionby aright-angled impedance wedge," *Radio Sci.*, Vol. 43, RS4S02, 2008.
13. Senior, T. B. A. and J. L. Volakis, *Approximate Boundary Conditions in Electromagnetics*, Stevenage, IEE, 1995.
14. Daniele, V. G. and G. Lombardi, "Wiener-Hopf solution for impenetrable wedges at skew incidence," *IEEE Trans. Antennas Propag.*, Vol. 54, 2472–2485, 2006.
15. Lyalinov, M. A. and N. Y. Zhu, "Diffraction of a skew incident plane electromagnetic wave by an impedance wedge," *Wave Motion*, Vol. 44, 21–43, 2006.
16. Holm, P. D., "A new heuristic UTD diffraction coefficient for nonperfectly conducting wedge," *IEEE Trans. Antennas Propag.*, Vol. 48, 1211–1219, 2000.
17. El-Sallabi, H. M. and P. Vainikainen, "Improvements to diffraction coefficient for non-perfectly conducting wedges," *IEEE Trans. Antennas Propag.*, Vol. 53, 3105–3109, 2005.
18. Nechayev, Y. I. and C. C. Constantinou, "Improved heuristic diffraction coefficients for an impedance wedge at normal incidence," *IEE Proc. — Microw. Antennas Propag.*, Vol. 153, 125–132, 2006.
19. Ferrara, F., C. Gennarelli, R. Guerriero, G. Riccio, and C. Savarese, "A UAPO diffraction contribution to take into account the edge effects in microstrip reflectarrays," *Electromagn.*, Vol. 26, 461–471, 2006.
20. Gennarelli, G. and G. Riccio, "Diffraction by a planar metamaterial junction with PEC backing," *IEEE Trans. Antennas Propag.*, Vol. 58, 2903–2908, 2010.

21. Gennarelli, G. and G. Riccio, "A uniform asymptotic solution for diffraction by a right-angled dielectric wedge," *IEEE Trans. Antennas Propag.*, Vol. 59, 898–903, 2011
22. Gennarelli, G. and G. Riccio, "Plane-wave diffraction by an obtuse-angled dielectric wedge," *J. Opt. Soc. Am. A*, Vol. 28, 627–632, 2011.
23. Gennarelli, G. and G. Riccio, "Useful solutions for plane wave diffraction by dielectric slabs and wedges," *Int. J. Antennas Propag.*, 1–7, 2012.
24. Gennarelli, G. and G. Riccio, "Diffraction by 90° penetrable wedges with finite conductivity," *J. Opt. Soc. Am A.*, Vol. 31, 21–25, 2014.
25. Gennarelli, G., M. Frongillo, and G. Riccio, "High-frequency evaluation of the field inside and outside an acute-angled dielectric wedge," *IEEE Trans. Antennas Propag.*, Vol. 63, 374–378, 2015.
26. Frongillo, M., G. Gennarelli, and G. Riccio, "Diffraction by a structure composed of metallic and dielectric 90° blocks," *IEEE Antennas Wireless Propag. Lett.*, Vol. 17, 881–885, 2018.
27. Frongillo, M., G. Gennarelli, and G. Riccio, "Plane wave diffraction by arbitrary-angled lossless wedges: High-frequency and time-domain solutions," *IEEE Trans. Antennas Propag.*, Vol. 66, 6646–6653, 2018.
28. Frongillo, M., G. Gennarelli, and G. Riccio, "Diffraction by a dielectric wedge on a ground plane," *Progress In Electromagnetics Research M*, Vol. 82, 9–18, 2019.
29. Gennarelli, G. and G. Riccio, "On the accuracy of the UAPO solution for the diffraction by a PEC — DNG metamaterial junction," *IEEE Antennas Wireless Propag. Lett.*, Vol. 19, 581–585, 2020.
30. Gennarelli, G. and G. Riccio, "High-frequency diffraction contribution by planar metallic — DNG metamatrial junctions," *Int. J. Microw. Wireless Tech.*, 1–6, 2020.
31. Frongillo, M., G. Gennarelli, and G. Riccio, "Useful solutions for the plane wave diffraction by a configuration of dielectric and metallic acute-angled wedges," *Int. J. Comm. Antennas Propag.*, Vol. 10, 68–75, 2020.
32. Meana, J. G., J. A. Martinez-Lorenzo, F. Las-Heras, and C. Rappaport, "Wave scattering by dielectric and lossy materials using the Modified Equivalent Current Approximation (MECA)," *IEEE Trans. Antennas Propag.*, Vol. 58, 3757–3760, 2010.
33. Meana, J. G., J. A. Martinez-Lorenzo, and F. Las-Heras, "High frequency techniques: The physical optics approximation and the Modified Equivalent Current Approximation (MECA)," *Electromagnetic Waves Propagation in Complex Matter*, A. Kishk (ed.), 207–230, Intech, Croatia, 2011.